

THE LUMINOSITY FUNCTION OF THE GLOBULAR CLUSTER NGC 6397 NEAR THE LIMIT OF HYDROGEN BURNING¹

IVAN R. KING², JAY ANDERSON², ADRIENNE M. COOL³, AND GIAMPAOLO PIOTTO⁴

Written 2021 November 4

ABSTRACT

Second-epoch *HST* observations of NGC 6397 have led to the measurement of proper motions accurate enough to separate the faintest cluster stars from the field, thus extending the luminosity function of this globular cluster far enough to approach the limit of hydrogen burning on the main sequence. We isolate a sample of 1385 main-sequence stars, from just below the turnoff down to $I = 24.5$ ($M_I \simeq 12.5$), which corresponds to a mass of less than $0.1 m_\odot$ for the metallicity of this cluster. Below $I = 22$ ($M_I \simeq 10$), the main-sequence luminosity function drops rapidly, in a manner similar to that predicted by theoretical models of low-mass stars near the hydrogen-burning limit.

Subject headings: Globular Clusters: Individual (NGC 6397) — Stars: Hertzsprung–Russell Diagram — Stars: Interiors — Stars: Low-Mass, Brown Dwarfs

1. INTRODUCTION

On the lower main sequence, there is a mass limit below which the center of a contracting protostar fails to reach the temperature needed for the hydrogen-burning nuclear reactions that characterize the life of a main-sequence star. At this limit of hydrogen burning, the stars of an otherwise smooth distribution of stellar masses divide between normal main-sequence stars, above, and brown dwarfs, below. The former shine continuously for much longer than a Hubble time, while the latter fade, so that after the >10 Gyr age of a globular cluster has passed, brown dwarfs are well separated in luminosity from hydrogen-burning stars (e.g., Burrows et al. 1993). Among the hydrogen-burning stars in the near neighborhood of the limit, theory predicts a steep decline in the luminosity function (LF), even before the more abrupt plunge of the LF when the limit is reached (e.g., D’Antona 1995, and other sources to be discussed below).

This limit should manifest itself particularly well in globular clusters, for three reasons: (1) The stars of a cluster have a common age and composition, and can be observed as a compact group. (2) At the low metal abundances of globular clusters, the hydrogen-burning limit occurs at a higher mass than for stars of solar metal abundance. (3) Stars of low metallicity are more luminous, at a given mass, than are those of high metallicity. It was for these reasons that Vittorio Castellani and Vittoria Caloi proposed to the European Space Agency in 1984 that the Hubble Space Telescope be used to look for the lower limit of hydrogen burning on the lower main sequences of the nearest globular clusters.

The cluster of smallest distance modulus is NGC 6397, for which we adopt $(m - M)_I \simeq 12.05$. Two WFPC2 observing

programs have been directed at the faint stars of this cluster (Paresce, De Marchi, & Romaniello 1995; Cool, Piotto, & King 1996 = CPK). Both studies showed a drop in the luminosity function below $I = 21$, but with weak statistics. As CPK emphasized, what was lacking was not a faint limiting magnitude, but rather the ability to distinguish the faintest cluster stars from the much more numerous field stars.

On encountering this frustration, however, we realized that the proper motion of NGC 6397 ($\simeq 15$ mas/yr [Cudworth & Hanson 1993]) is large enough that a repeat of our 1994 exposures should allow a proper-motion separation of individual cluster members from field stars. We therefore re-imaged the cluster in 1997. We expected a mean cluster motion of over 0.4 pixel, with the internal velocity dispersion of the cluster contributing a little over 0.01 pixel scatter.

2. OBSERVATIONS

For various observational reasons, the 1994 exposures had covered an irregular pattern (CPK, Fig. 1). For the second-epoch we chose two pointings that maximize the number of stars covered by at least three orbits at each epoch. They include about 88% of the 2770 stars measured by CPK. The second-epoch exposures were made with the F814W filter on June 4, 1997.

The first-epoch exposures had been dithered by circumstance; those of the second epoch were deliberately placed at three different fractional-pixel positions within each of the two major pointings. Each dither position was held for one full orbit, which was divided into three exposures of 700–800 s each, and one short exposure of 60 s.

Individual images were cleaned of cosmic rays by intercomparison with one another, and the long exposures of each orbit were then averaged. The result was six single-orbit images, consisting of three dithers at each of two pointings.

The basic aim of the astrometry was to establish which of the faint stars shared the motion of the cluster and which did not. For each star measured in the first epoch, we used the first- and second-epoch positions of the nearest ten or so bright cluster members (i.e., stars with $I < 22$ and $V - I$

¹Based on observations with the NASA/ESA *HubbleSpaceTelescope*, obtained at the Space Telescope Science Institute, which is operated by AURA, Inc., under NASA contract NAS 5-26555.

²Astronomy Department, University of California, Berkeley, CA 94720–3411; king@glob.berkeley.edu, jay@cuspl.berkeley.edu

³Department of Physics and Astronomy, San Francisco State University, 1600 Holloway Avenue, San Francisco, CA 94132; cool@sfsu.edu

⁴Dipartimento di Astronomia, Università di Padova, Vicolo dell’Osservatorio 5, I–35122 Padova, Italy; piotto@astrpd.pd.astro.it

within 0.05 mag of the main-sequence ridge line), to determine the presumed location of the target star in each of the second-epoch images.

We then searched for a star at this position. If the star had the same proper motion as the cluster stars, we would expect to find it in the predicted location. Any difference of motion from that of the cluster should manifest itself by an offset from this location. We measured positions for the brighter stars ($I \lesssim 24$) by least-squares PSF-fitting. For faint stars we determined a center from a $+$ -shaped set of 5 pixels centered on the star's brightest pixel, using a PSF-based algorithm that will be described in a later paper. The level of accuracy of our astrometry will be indicated by the scatter in the measured motions of the cluster stars, all of whose true motions should be nearly zero in the system described.

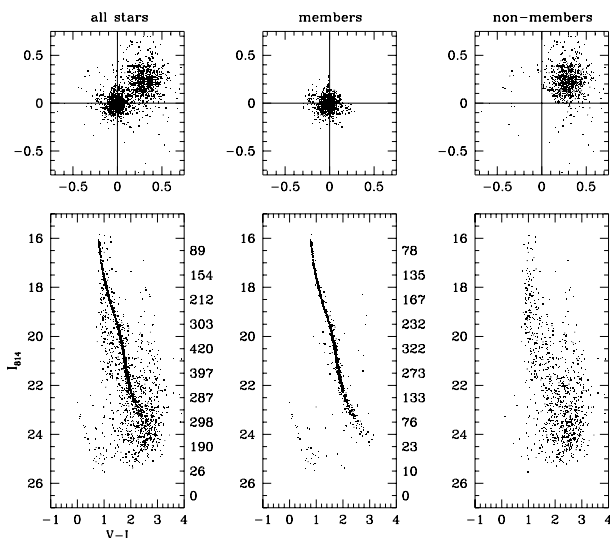


Figure 1. Proper-motion distributions, above, and color-magnitude diagrams, below. The scale of the proper motions is displacement in WFC pixels over the 32-month time baseline; a full WFC pixel of displacement would correspond to 37.5 mas/yr. Since all reference stars were cluster members, the zero point of motion is the mean motion of cluster stars. Left: the entire sample; center: stars within the proper-motion region described in the text; right: stars outside this region. Numbers at right are stars per unit-magnitude bin.

3. RESULTS AND DISCUSSION

In Figure 1 we show the distribution of proper motions and the color-magnitude diagram (CMD) for the entire sample, as well as for two subsets of stars, divided according to whether the proper motion of a star falls inside or outside of a boundary in the proper-motion diagram that approximately isolates the cluster members. For this boundary we chose a radius of 0.15 pixel in the quadrant that contains most of the field stars and 0.3 pixel in the other three quadrants. These radii were chosen by trial and error so as to achieve the best easy separation between cluster members and field stars.

The success of the separation is immediately evident. It is not perfect, of course, because (1) the error distribution causes some cluster members to fall outside the circle, and (2) the proper motions of the field stars fall all over the

graph, so that inevitably some field stars have motions that are close to that of the cluster.

In the cluster-member CMD in Figure 1 the number of cluster stars is dropping off sharply below $I = 23.5$ (see also Fig. 2), and this is not purely incompleteness, since the non-member set is full of stars at least to $I = 24.5$. In fact, the completeness figures are already known, since the stars studied here are those of the first-epoch study (CPK), where thorough completeness tests were carried out. At $I = 23.5$ our completeness is 90%, and it is still 78% at $I = 24.5$ (*cf.* Table 1). As nearly every epoch-1 star within the field of view of the second-epoch observations was recovered (see below), these completeness figures still apply.

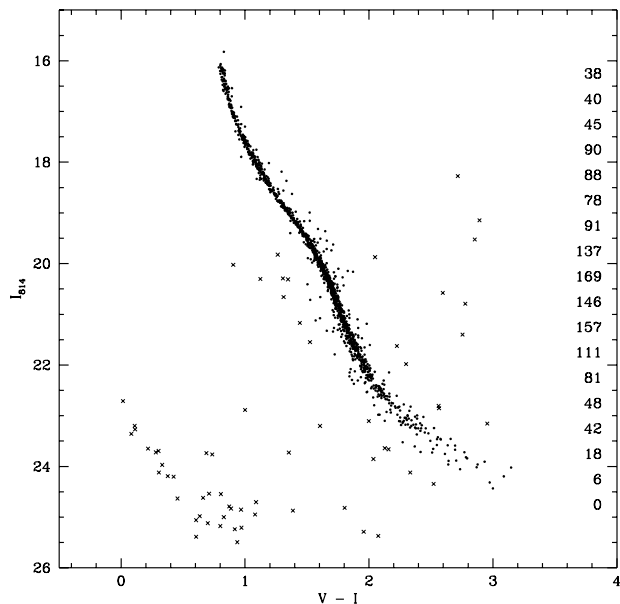


Figure 2. Blow-up of bottom center panel of Fig. 1, with counts per half-magnitude interval tallied at the right. Dots: stars within 0.2 mag of the color of the main-sequence ridge line (only these are counted in the luminosity function); crosses: stars outside this color range.

Figure 2 is a blowup of the CMD of the cluster sample in Fig. 1; stars whose colors fall within 0.2 mag of the main-sequence ridge line are plotted as filled circles and are considered to be cluster members. For the brighter stars this color criterion is overly generous and errs in the direction of allowing some field stars into the sample. (It also allows for the possibility of a population of cluster binaries to the right of the main sequence—a question to which we shall return in a later paper.) For the fainter stars, however, where the photometric errors increase, it insures that cluster stars are not lost outside a color range that is too narrow. Because of the preponderance of field stars at the faint end, even though an occasional cluster star may be missed there, the net error goes in the direction of making the drop-off of the number of cluster stars *less* steep.

Another concern is the possibility that faint cluster members are lost astrometrically, as an increasing measurement error pushes them beyond the proper-motion separation criterion. We examined the overall distribution of proper motions as a function of magnitude. Figure 3 shows the inner

part of this distribution in the faintest four 1-mag intervals. The spread of apparent proper motions of cluster stars does increase somewhat with faintness, but very few of them should be lost by the separation criterion that was used. In the $I = 24$ to 25 interval, we examined each individual star that lies between the solid arc and the dashed arc (at radius 0.25) in the first quadrant; two of the eight actually fall just within our color limits, but the color distribution of the eight is spread in a way that is consistent with these two being just the red tail of a field-star distribution.

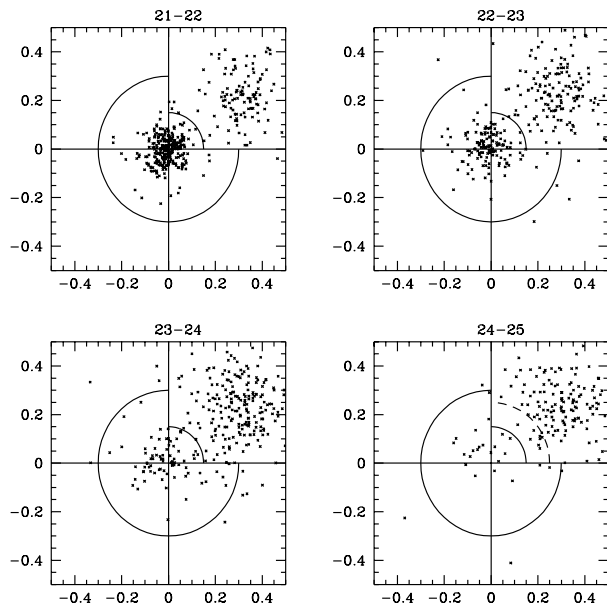


Figure 3. Proper motions in each of our faintest four unit intervals of I magnitude. The arcs show our separation criterion between cluster and field; the dashed arc is explained in the text.

In order to convert the numbers at the right edge of Fig. 2 to a luminosity function, we need careful completeness corrections. Our present list is the stars of the first-epoch study, whose completeness was studied by CPK. In Table 1 we give the full results of the completeness tests made for that study. In principle, an additional correction might

Table 1. Completeness.

I	Fraction	I	Fraction
16.50	1.00	23.50	0.90
17.50	1.00	24.00	0.87
18.50	1.00	24.25	0.85
19.50	0.98	24.50	0.78
20.50	0.97	24.70	0.68
21.50	0.96	24.90	0.45
22.50	0.93	25.00	0.35

be needed for stars missed in the second-epoch astrometric study, where we included only stars that were identified and measured in all three orbits of at least one of the two pointings. But this loss was almost purely geometric (the coverage was 88% of the previous field); in the area covered by the

second-epoch images, only 27 stars out of 2438 were missed, and these were distributed fairly evenly over magnitude.

Our new LF is plotted in the upper part of Figure 4. It agrees well with the earlier CPK points, except for the last of the latter, which was affected by the very field contamination that we are removing here. We note that we showed in a previous paper (King, Sosin, & Cool 1995) that the field we have studied is at a distance from the cluster center where, fortuitously, the local LF should be very similar to the cluster's global LF.

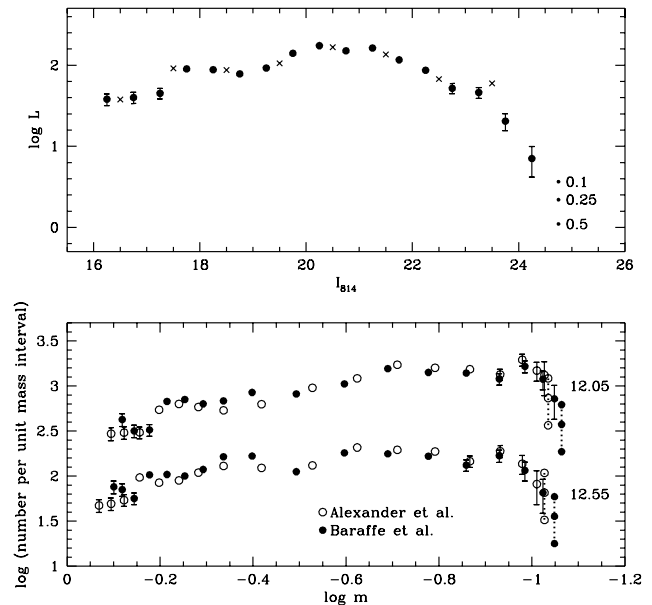


Figure 4. (top) Our new luminosity function of NGC 6397, with Poisson error bars (plotted only when they are larger than the sizes of the symbols). The vertical array of three small dots is explained in the text. The crosses are the LF given by CPK, converted to the present field size. (bottom) Mass functions, as derived from each of the two MLRs indicated. For clarity the sets of 3 points representing the empty bin have been connected with lines. The error bars arise from those of the log LF points. The MFs are shown for two different assumed distance moduli, as labeled.

A problem is posed, in plotting the LF, by the fact that our faintest half-magnitude bin has no observed cluster stars; the statistical interpretation of a zero count is always a problem. What we have done is to ask, for various putative values of the LF at $I = 24.75$, what the probability would be of our observing a count of zero in this bin. The points plotted are such that if the true value of the LF were at that point, the probability of observing zero stars in that bin would be, respectively, 0.1, 0.25, and 0.5, for the three points plotted. The results suggest that it is quite unlikely that this bin fails to accentuate the steep plunge of the LF.

We should caution against over-interpreting this zero-count bin, however. As Table 1 shows, over the magnitude range of this bin ($I = 24.5$ to 25.0) the completeness of the sample drops from 0.78 to 0.35. We have consequently been re-examining our images, to see if we can possibly find additional main-sequence cluster members in this range. This study will not be complete for some time, but it seems not

unlikely that our field will yield up a star or two that is below $I = 24.5$ and is on the cluster main sequence. Even so, the LF would be dropping *very* rapidly at this magnitude.

We now turn to theoretical studies of stellar structure, in order to see how the drop-off in our new LF compares to what is expected just above the limit of hydrogen burning, from current models of these low-metallicity stars ($[\text{Fe}/\text{H}] \simeq -1.9$ [Djorgovski 1993]). We do this by using theoretical mass–luminosity relations (MLRs) to derive the mass function (MF) that is implied by our LF. In principle, if the MLR is correct, the resulting MF should behave smoothly near the H-burning limit, because the process of star formation should be unaware of the later restrictions imposed by the physics of energy generation. Though fundamentally qualitative, this smoothness criterion is a potentially sensitive test. Because of the way that the LF maps into the MF, there will be an abrupt feature in the MF unless the steep drop in the LF is matched by a comparably steep rise in the MLR slope, by which the LF is multiplied in order to convert it into an MF.

We have derived MFs using two values of the I distance modulus, and two different MLRs. The latter are derived from stellar models which have been shown by their authors (Alexander et al. 1997, Baraffe et al. 1997) to give a satisfactory fit to the CPK main-sequence ridge line in NGC 6397. In examining the MFs, however, it should be kept in mind that these two sets of models are characterized not only by different underlying physics, but also by different assumed chemical compositions. As for the distance modulus, because its value controls the alignment of the theoretical slopes with the observed points, it can have a significant impact on the resulting MF (D’Antona 1998). The distance moduli of 12.05 and 12.55 that we have chosen bracket the range in which the true value is likely to lie.

The results are shown in the lower half of Fig. 4. The broad features of the MFs are similar in all cases, rising gradually and then leveling off at low masses. There are indications of features in the MFs near $\log m = -.015$ – 0.2 and -0.45 . The former region, however, is close to the main-sequence turnoff, where the MLR is sensitive to age and evolution. Both features will be discussed elsewhere, along with the extensive LF material that is available on other clusters (as, for example, in Piotto, Cool, & King [1997], where we give our previous LF values along with those for three other clusters).

Here our focus is on the low-mass region. It is noteworthy that the striking drop at the faint end of the luminosity function is essentially absent in the MF. The steepness of the theoretical mass–luminosity relation near the H-burning

limit has largely compensated for it, raising the MF up to be nearly flat below $\log m \sim -0.7$. In the last two occupied bins we see some indication of a turn-down, with the empty bin accentuating this effect. This takes place within a mass range of only a little over $0.01 m_{\odot}$. But because the amount of turn-down hardly exceeds the size of the error bars, and because of the even larger uncertainty associated with the empty bin, the present study cannot determine with any confidence whether or not the MF begins to drop below $\log m \sim -1.0$. Any sudden turn-down of the MF within a small mass range would be surprising; it would be of great interest if it were a real feature of the MF, or it could equally well indicate that the MLRs do not have a steep enough slope in this region. Thus improved data for the now-empty last bin could be quite significant. Also needed are study of a larger sample within NGC 6397, and examination of other clusters of small distance modulus.

4. SUMMARY

The main-sequence luminosity function that we present for NGC 6397 reaches into the mass range immediately above the limit of hydrogen burning. Our results demonstrate that *HST* proper motions can be very effective in distinguishing cluster stars from the field. The newly derived LF is no longer subject to the uncertainties associated with field stars that limited previous studies of this cluster, and extends to faint enough magnitudes to include stars with masses below $0.1 m_{\odot}$. We use mass–luminosity relations from theoretical studies to convert our LF into an MF, and find that the resulting MF is reasonably smooth down to $0.1 m_{\odot}$. Statistical uncertainties limit what can be gleaned about the MF at even lower masses,

In future months we will refine all of the measurements and calculations that have gone into this brief Letter, in order to present as accurate a delineation of the lower main sequence of NGC 6397 as we can. We believe, however, that even the present preliminary results are of interest, showing for the first time the neighborhood of the lower limit of hydrogen burning on the main sequence of a globular cluster.

We are grateful to the Teramo group (Alexander et al. 1997) and the Lyon group (Baraffe et al. 1997) for communication of data prior to publication. We also gratefully acknowledge helpful discussions of the stellar models with Francesca D’Antona, Lars Bildsten, Santi Cassisi, and Gilles Chabrier. This work was supported by NASA grant GO-6797 from STScI (IRK, JA, and AMC), as well as by the Agenzia Spaziale Italiana and the Ministero dell’Università e della Ricerca Scientifica e Tecnologica (GP).

REFERENCES

- Alexander, D. R., Brocato, E., Cassisi, S., Castellani, V., Ciacio, F., & Degl’Innocenti, S. 1997, *A&A*, 317, 90
 Baraffe, I., Chabrier, G., Allard, F., & Hauschildt, P. H. 1997, *A&A*, in press (Nov. 1997)
 Burrows, A., Hubbard, W. B., Saumon, D., & Lunine, J. I. 1993, *ApJ*, 406, 158
 Cool, A. M., Piotto, G., & King, I. R. 1996, *ApJ*, 468, 655.
 Cudworth, K. M., & Hanson, R. B. 1993, *AJ*, 105, 168
 D’Antona, F. 1995, in *The Bottom of the Main Sequence — and Beyond*, ed. C. G. Tinney (Berlin: Springer), p. 13
 D’Antona, F. 1998, in *The Stellar Initial Mass Function*, ed. G. Gilmore, ASP Conference Series, in press
 Djorgovski, S. G. 1993, in *Structure and Dynamics of Globular Clusters*, eds. S. G. Djorgovski & G. Meylan (San Francisco: ASP), p. 373
 Holtzman, J., et al. (18 authors). 1995, *PASP*, 107, 156
 King, I. R., Sosin, C., & Cool, A. M. 1995, *ApJ*, 452, L33
 Paresce, F., De Marchi, G., & Romaniello, M. 1995, *ApJ*, 440, 216
 Piotto, G., Cool, A. M., & King, I. R. 1997, *AJ*, 113, 1345.